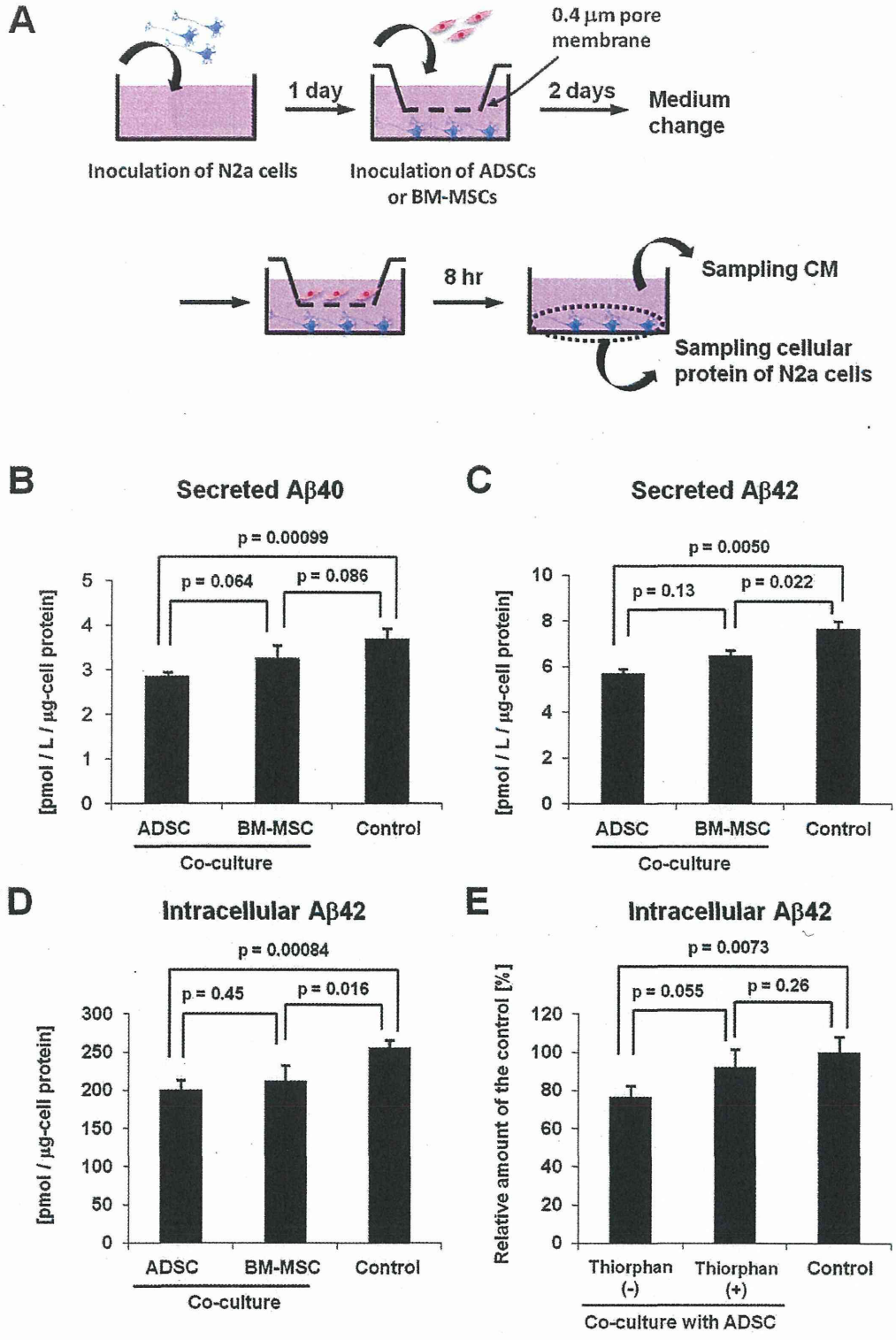

Figure 5 | ADSCs decrease both the extracellular and intracellular Aβ levels of N2a cells. (A) Schematic representation of the co-culture experiments of N2a cells with ADSCs or BM-MSCs using cell culture inserts. Secreted Aβ40 (B) and Aβ42 (C) levels were measured using the collected CM in the bottom chambers by ELISA. Each value was normalized to the protein content of N2a cell lysates. Data are the mean ± S.D. (n = 4). (D) Intracellular Aβ42 levels were measured using the N2a cell lysates by ELISA. Each value was normalized to the protein content of N2a cell lysates. (E) Intracellular Aβ42 levels were compared in co-cultures of ADSCs and N2a cells in the presence and absence of thiorphan. Each value is shown as the relative level to the control. Data are the mean ± S.D. (n = 4).

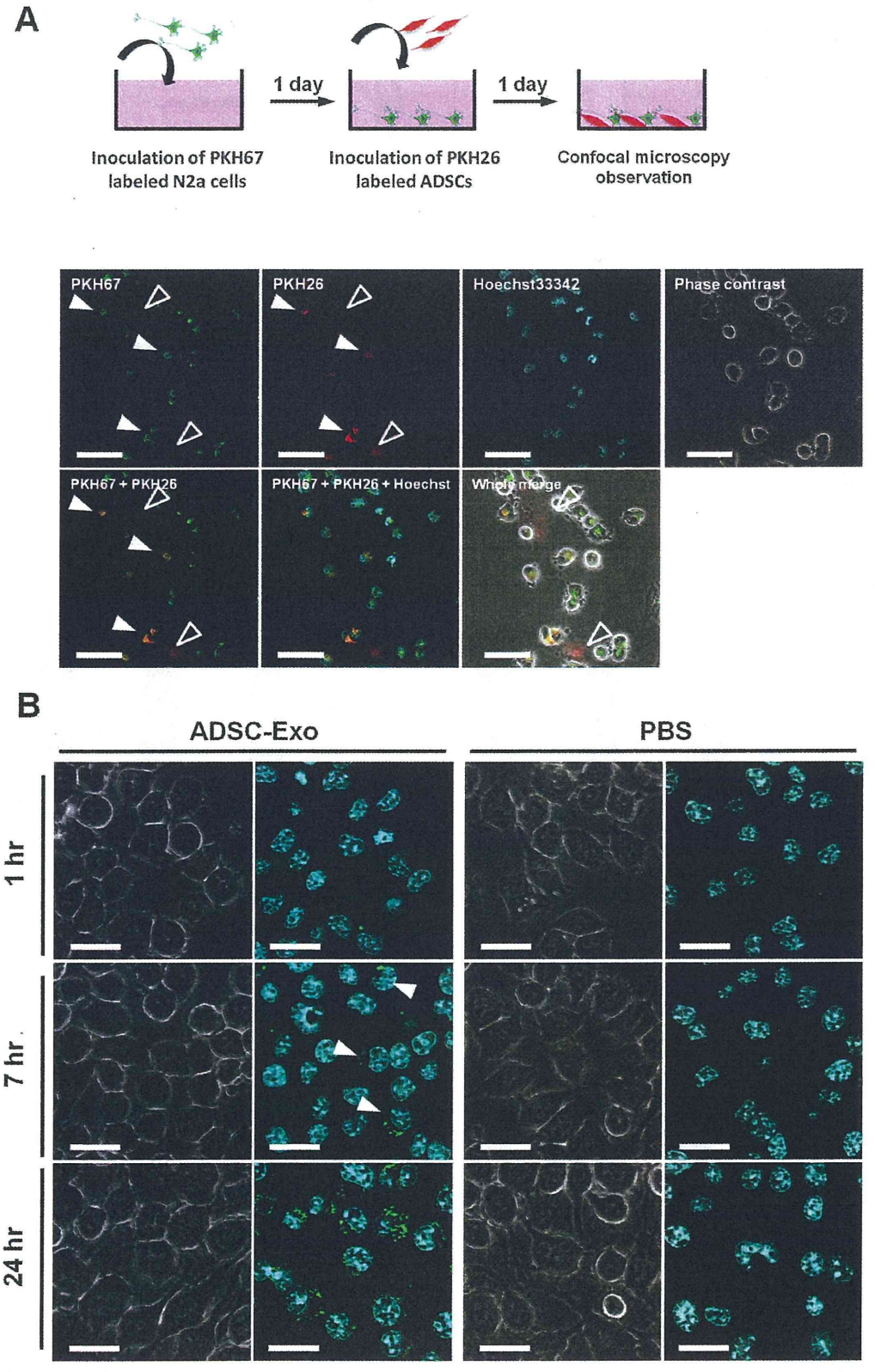

Figure 6 | ADSC-derived exosomes are incorporated into N2a cells. (A) Top diagram shows the schematic representation of the co-culture experiements of N2a cells and ADSCs labeled with PKH67 and PKH26, respectively. Bottom diagram shows the representative image taken 24 hr after co-culture of N2a cells with ADSCs. Filled arrowheads indicate N2a cells co-stained with PKH26 and PKH67. Open arrowheads indicate PKH26 labeled ADSCs. Scale bar: 50 μm. (B) Purified ADSC exosomes or vehicle PBS(-) as a control were labeled with PKH67, and incubated with cultured N2a cells. 7 hr after incubation, some of the cells were stained green (arrowheads). After 24 hr, most N2a cells were stained green. Scale bar: 25 μm.

Discussion

In this study, we demonstrated the unique potential of ADSCs for AD treatment. The main finding was that ADSCs secreted functional NEP in association with exosomes. Most importantly, these ADSC-derived exosomes exhibited NEP-specific enzyme activity. Furthermore, it was indicated that exosomes secreted by ADSCs were transferred to N2a cells, and contributed, at least in part, to decrease of both extracellular and intracellular Aβ levels. Another important observation was that ADSCs expressed NEP at a higher level than BM-MSCs. These results suggest that ADSCs may serve as a promising cell source for exosome-based AD treatments.

To our knowledge, this is the first report of the isolation of exosomes containing functional NEP from cultured cells, suggesting a promising new approach for AD treatment. Earlier studies have shown that NEP is present in microvesicles derived from certain body fluids, including prostatic fluid[34], epididymal fluid[35], and urine[36]. However, no study has focused on the therapeutic potential of microvesicle-bound NEP for AD. Indeed, it seems impractical to obtain a sufficient amount of microvesicles from the limited amount of available body fluid. In this context, MSCs have a great advantage because they can be isolated in large amounts from patients and they have the ability to expand many-fold in culture. Importantly, the co-culture experiments suggested that ADSC-derived exosomes contributed to decrease of the secreted Aβ level in N2a cells. Furthermore, it is intriguing that the intracellular Aβ42 level was also decreased by co-culture with ADSCs as well as by addition of ADSC-derived exosomes. Although we do not exclude other possible effects of ADSCs on the co-cultured N2a cells, the results indicate a novel possibility: that is, incorporated ADSC-derived exosomes contributed to the degradation of the intracellular Aβ42 in the recipient N2a cells. Many reports have suggested that accumulation of intraneuronal Aβ42 is an early event in the progression of AD, preceding the formation of extracellular Aβ deposits[37]. Thus, our results suggest the possibility that ADSC-derived exosomes contribute to prevention of extracellular plaque formation and subsequent AD pathogenesis.

Our results also demonstrated that ADSCs, but not BM-MSCs, expressed enzymatically active NEP. Since the discovery of MSCs in bone marrow, MSCs have been identified in many adult tissues[8–10]. Although ADSCs and BM-MSCs are considered to be similar, an increasing number of reports have indicated that these cells have phenotypic differences regarding differentiation capacity[8], immunosuppressive potential[38,39], homing and migratory behavior[40], and trophic effects[39,41]. These observations highlight the importance of selecting the optimal mesenchymal tissue as a source of MSCs for specific purposes. In this context, our comparative analyses between ADSCs and BM-MSCs provide strong evidence that ADSCs are the more suitable source of NEP-bound exosomes.

Another interesting finding was that ADSC-derived exosomes were rich in NEP. The fluorogenic substrate used in the present study can be cleaved by NEP and closely related enzymes, including IDE, ECEs, and ACEs. All of these enzymes can degrade Aβ, although their contribution in Aβ clearance in the brain is small[4,5]. ECEs and ACEs are membrane-bound enzymes, suggesting their potential presence on secreted exosomes. However, the experiments with the NEP-specific inhibitor thiorphan revealed that ~ 90% of the enzyme activity of ADSC-derived exosomes was accounted for by NEP; the counterpart of the donor ADSC lysates was ~ 40%. Furthermore, we also found that BM-MSC-derived exosomes also exhibited NEP-specific activity. Intriguingly, whereas NEP-specific activity of parental BM-MSCs slightly contributed to the total enzyme activity, that of their exosomes accounted for more than 70% of the total enzyme activity (Fig. S6). We do not have an explanation for these observations, but it is likely that NEP was enriched in exosomes during their biogenesis. Collectively, these results suggest that ADSC-derived exosomes offer a new therapeutic approach to AD.

Recent reports support a scenario in which NEP-loaded exosomes contribute to Aβ clearance in the brain. A major obstacle for systemically administered drugs is the blood-brain barrier (BBB). Membrane vesicles have been proposed to be transported across the interior of a cell via transcytosis[42], which may enable these vesicles to cross the BBB. Indeed, recent reports have suggested that exosomes administered intravenously[43] or intranasally[44] crossed the BBB and resulted in successful delivery of the cargo directly into the brain. These studies strongly support the hypothesis that ADSC-derived exosomes can directly enter the brain and help clear extracellular Aβ. Another possibility is that ADSC-derived exosomes may help lower peripheral Aβ levels, which possibly promotes brain Aβ clearance. Peripheral degradation of Aβ through virus-mediated NEP gene delivery has been demonstrated to decrease brain soluble Aβ peptide levels[45,46]. In this context, NEP delivery using ADSC-derived exosomes has an advantage in patient safety because it does not require the use of viral vectors. Taken together, ADSC-derived exosomes may offer a promising approach to NEP delivery peripherally and/or directly into the brain.

In conclusion, this study proposes a new therapeutic approach to AD using ADSC-derived exosomes. Further work will be required to assess the utility of NEP-loaded exosomes for AD therapy.

Methods

Cell culture. ADSCs #1–3 were purchased from Invitrogen. ADSCs #4–6 were isolated in our laboratory by processing adipose tissue as previously described[11]. BM-MSCs #1–3 and #4 were purchased from the RIKEN cell bank and Cambrex, respectively. The donor information for ADSCs and BM-MSCs is listed in Supplementary Tables 1 and 2, respectively. BM-MSCs and ADSCs were routinely cultured in reduced serum (2%) medium (MesenPRO RS, Invitrogen) containing 1 × Glutamax (Invitrogen) and 1 × antibiotic antimycotic (Invitrogen). All ADSCs and BM-MSCs were used within the eighth passage. Stable mouse neuroblastoma N2a cells expressing both human APP695 with the Swedish mutation and presenilin 2 with the N141I mutation were kindly provided by Dr. Saido Takaomi (RIKEN Brain Institute, Japan). N2a cells were cultured in Dulbecco's modified Eagle's medium (Invitrogen) supplemented with 10% FBS (Invitrogen) and 1 × antibiotic antimycotic.

Flow cytometry. Aliquots of detached cells were washed in PBS containing 2% BSA and stained with anti-CD10 PE-conjugated (Biolegend). Samples were acquired using Cytomics FC500 flow cytometer (Beckman Coulter) and analyzed by CXP and WinMDI software.

Quantitative reverse transcription PCR (qRT-PCR). Total RNA was isolated from ADSCs and BM-MSCs with the RNeasy Mini Kit (QIAGEN). Reverse-transcription was performed using SuperScript III Reverse Transcriptase (Invitrogen, Tokyo, Japan) and random primers (Invitrogen) according to the manufacturer's guidelines. cDNAs were used for PCR utilizing Platinum SYBR Green qPCR SuperMix UDG (Invitrogen). NEP expression levels were normalized to an endogenous control, β-actin. The sequences of the NEP and β-actin primers (Invitrogen) were as follows: for NEP, 5′-CCTTCTTTAGTGCCCAGCAG-3′ (forward) and 5′- TGAGTCC ACCAGTCAACGAG-3′ (reverse); for β-actin, 5′- ACTCTTCCAGCCTTCC TTCC-3′ (forward) and 5′- AGCACTGTGTTGGCGTACAG-3′ (reverse).

Protein extraction. ADSCs and BM-MSCs were dissolved in Mammalian Protein Extraction Reagent (M-PER) (Pierce, Rockford, IL). Prepared cell lysates were used for immunoblotting and NEP enzyme activity assays. The protein concentrations were measured by the Bradford method using a protein assay kit (Bio-Rad).

Immunoblot analysis. Cell lysates and exosomes were separated on SDS-polyacrylamide gels and transferred to polyvinylidine difluoride membranes (BIORAD, Tokyo, Japan). Blots were blocked in blocking solution (Nacalai Tesque) at 4°C overnight and incubated at room temperature for 1 hour with mouse monoclonal anti-NEP (Abcam) (1 : 1000), mouse anti-actin (1 : 2000), mouse-anti CD63 (BD) (1 : 200), mouse-anti CD81 (Santa Cruz Biotechnology) (1 : 200), or mouse-anti cytochrome-c (BD) (1 : 200) antibody (CD63 was assessed under nonreducing conditions). Following washing in TBS-T, the membranes were incubated for 1 hour with sheep anti-mouse IgG-HRP-linked whole antibodies. Bound antibodies were visualized by chemiluminescence using an ECL Plus Western blotting detection system (RPN2132) (GE HealthCare) or an ImmunoStar kit (Wako), and images were analyzed by a LuminoImager (LAS-3000; Fuji Film, Inc.).

Immunocytochemistry. The cells were cultured in glass base dishes (IWAKI), and subsequently fixed in 4% paraformaldehyde (Sigma-Aldrich) in PBS. Heat-induced antigen retrieval was performed using ImmunoSavor (Nisshin EM Co. Ltd.). After incubation in blocking solution (Nacalai Tesque), the cells were incubated with

mouse monoclonal anti-NEP (Abcam) at 1 : 100 overnight at 4°C. Then, the cells were incubated with Alexa Fluor 488-conjugated goat anti-mouse IgG antibody (Invitrogen) at 1 : 500 for 60 min. Nuclei were counterstained with Hoechst 33342 (Dojindo).

Preparation of conditioned medium (CM) and exosomes. Prior to culture medium collection, ADSCs were washed twice with PBS, and the medium was switched to fresh serum-free medium (StemPRO SFM, Invitrogen). After incubation for 2–3 days, the medium was collected and centrifuged at 2,000 × g for 15 min at room temperature. The cells were supplemented with fresh SFM, cultured for 2–3 more days, and the medium was collected and centrifuged as described above. The harvested media were combined into 1 batch. To thoroughly remove cellular debris, the supernatant was filtered with a 0.22-μm filter unit (Millipore). Then, the CM was ultracentrifuged at 110,000 × g for 70 min at 4°C. The pellets were washed with 11 ml PBS, and after ultracentrifugation, they were resuspended in PBS. The exosome fraction protein content was assessed by the Bradford method.

NEP enzyme activity assay. Neprilysin activity was determined by fluorescence resonance energy transfer. The fluorogenic peptide substrate Mca-RPPGFSAFK(Dnp)-OH (R&D Systems, Inc.) was added at a final concentration of 20 μM to 5 μg cell lysates, and 5 or 10 μg ADSC-derived exosomes, respectively. The enzymatic reaction was carried out at 37°C in the presence or absence of the NEP inhibitor thiorphan (2.5 μg/mL) (Enzo Life Science). Fluorescent intensity was read at excitation and emission wavelengths of 320 nm and 405 nm, respectively, in kinetic mode for 5 minutes using a Safire Multi-Detection Monochrometer Microplate Reader (Tecan). The NEP-specific activity was determined as the fluorescence difference occurring in the presence or absence of thiorphan. NEP-specific or total enzyme activity rate was determined as the gradient of the corresponding time course of the fluorescent intensity. Then, the NEP contribution ratio was calculated as the percentage ratio of the NEP-specific activity rate and the total activity rate. We also quantified absolute NEP-specific activity using serial dilutions of recombinant human NEP (rhNEP) (R&D Systems, Inc.) as a standard. The gradient of the time course of the fluorescent intensity in its linear region was determined at each concentration of the rhNEP dilution series to produce a standard curve. NEP activity per sample protein amount was determined as the rhNEP-equivalent amount, which we termed as the "NEP activity index" with the unit ng-rhNEP/μg-sample protein.

Phase-contrast transmission electron microscopy. ADSC-derived exosomes were visualized by Terabase Inc. using the phase-contrast transmission electron microscopy, which can envision the high-contrast images of nano structures of soft-materials including biological samples such as liposomes, viruses, bacteria, and cells, without staining process which may cause damages on the subjects. The natural structure of the sample distributed in the solution can be observed by preparing the sample with rapid vitreous ice embedding method and using cryo phase-contrast transmission electron microscopy.

Measurement of size distribution and particle number by nanoparticle tracking analysis (NTA). NTA was carried out using the Nanosight system (NanoSight) on exosomes resuspended in PBS at a concentration of approximately 500 μg protein/mL and were further diluted 100-fold for analysis. The system focuses a laser beam through a suspension of the particles of interest. These are visualized by light scattering using a conventional optical microscope aligned perpendicularly to the beam axis, which collects light scattered from every particle in the field of view. A 60 s video records all events for further analysis by NTA software. The Brownian motion of each particle is tracked between frames, ultimately allowing calculation of the size through application of the Stokes-Einstein equation.

Size distribution analysis by scanning ion occlusion sensing (SIOS). SIOS analysis was carried out using the qNano system (Izon Science, Ltd.) on exosomes resuspended in PBS. SIOS allows single particle measurements as colloids and/or biomolecular analytes are driven through pores one at a time. Particles crossing the nanopore are detected as a transient change in the ionic current flow, which is denoted as a blockade event with its amplitude as the blockade magnitude. As blockade magnitude is proportional to particle size, accurate particle sizing can be achieved after calibration with a known standard.

Co-culture of N2a cells with ADSCs. For assessing whether MSCs can affect production and secretion of Aβ by N2a cells, we performed co-culture experiment using cell culture inserts possessing 0.4 μm pores (BD Falcon). N2a cells were seeded to the bottom chambers of 24 well-plates (BD Falcon) at 2×10^4 cells/well. On the next day, ADSCs #2 were seeded to the top chambers at 6×10^3 cells/insert which gave an almost confluent monolayer. After 2 days, culture media in the both top and bottom chambers were changed with fresh media, and the cells were cultured for further 8 hr. Then, the media in the bottom chambers were collected, centrifuged at 2,000 × g for 10 min, and the supernatants were used for the subsequent analysis. N2a cell lysates were also collected using M-PER, and cellular protein amounts were determined by Bradford method. Secreted and intracellular Aβ40 and 42 levels were measured using the CM and the N2a cell lysates, respectively, with ELISA kits (Wako). Both secreted and intracellular Aβ levels were normalized by the protein content of N2a cells. To investigate whether the decrease of Aβ levels was ascribed to NEP activity, thiorphan was added to the culture inserts at the concentration of 20 μM.

Exosome transfer analysis by co-culture experiments. N2a cells were labeled with a PKH67 green fluorescent labeling kit (Sigma-Aldrich) following the manufacture's instruction, and seeded to 35 mm glass base dishes (IWAKI) at 5×10^4 cells/dish. On the next day, ADSCs #2 were labeled with a PKH26 red fluorescent labeling kit (Sigma-Aldrich) and added to the dishes at 5×10^4 cells/dish (Fig. 5A). After 24 hr, cells were observed under confocal microscopy.

PKH67-labeled exosome transfer. Purified exosomes derived from ADSCs #2 CM were labeled with PKH67. Exosomes were incubated with 2 M PKH67 for 5 min, washed 4 times using a 100-kDa filter (Microcon YM-100, Millipore) to remove excess dye, and incubated with N2a cells cultured in 35 mm glass base dishes (Fig. 6A). Exosome-free PBS(-) that received the same treatment as above was used as a control. The cells were observed at 1, 7, and 24 hr under confocal microscopy.

1. Hardy, J. Amyloid, the presenilins and Alzheimer's disease. *Trends Neurosci.* **20**, 154–159 (1997).
2. Selkoe, D. J. The cell biology of beta-amyloid precursor protein and presenilin in Alzheimer's disease. *Trends Cell Biol.* **8**, 447–453 (1998).
3. Iwata, N., Higuchi, M. & Saido, T. C. Metabolism of amyloid-beta peptide and Alzheimer's disease. *Pharmacol. Ther.* **108**, 129–148 (2005).
4. Iwata, N. *et al.* Metabolic regulation of brain Abeta by neprilysin. *Science* **292**, 1550–1552 (2001).
5. Iwata, N. *et al.* Identification of the major Abeta1-42-degrading catabolic pathway in brain parenchyma: suppression leads to biochemical and pathological deposition. *Nat. Med.* **6**, 143–150 (2000).
6. Yasojima, K., Akiyama, H., McGeer, E. G. & McGeer, P. L. Reduced neprilysin in high plaque areas of Alzheimer brain: a possible relationship to deficient degradation of beta-amyloid peptide. *Neurosci. Lett.* **297**, 97–100 (2001).
7. Miners, J. S., Barua, N., Kehoe, P. G., Gill, S. & Love, S. Aβ-degrading enzymes: potential for treatment of Alzheimer disease. *J. Neuropathol. Exp. Neurol.* **70**, 944–959 (2011).
8. Sakaguchi, Y., Sekiya, I., Yagishita, K. & Muneta, T. Comparison of human stem cells derived from various mesenchymal tissues: superiority of synovium as a cell source. *Arthritis Rheum.* **52**, 2521–2529 (2005).
9. Banas, A. *et al.* Adipose tissue-derived mesenchymal stem cells as a source of human hepatocytes. *Hepatology* **46**, 219–228 (2007).
10. Chamberlain, G., Fox, J., Ashton, B. & Middleton, J. Concise review: mesenchymal stem cells: their phenotype, differentiation capacity, immunological features, and potential for homing. *Stem Cells* **25**, 2739–2749 (2007).
11. Banas, A., Yamamoto, Y., Teratani, T. & Ochiya, T. Stem cell plasticity: learning from hepatogenic differentiation strategies. *Dev. Dyn.* **236**, 3228–3241 (2007).
12. Sadan, O., Melamed, E. & Offen, D. Bone-marrow-derived mesenchymal stem cell therapy for neurodegenerative diseases. *Expert. Opin. Biol. Ther.* **9**, 1487–1497 (2009).
13. Jin, H. K., Bae, J. S., Furuya, S. & Carter, J. E. Amyloid beta-derived neuroplasticity in bone marrow-derived mesenchymal stem cells is mediated by NPY and 5-HT2B receptors via ERK1/2 signalling pathways. *Cell Prolif.* **42**, 571–586 (2009).
14. Habisch, H. J. *et al.* Efficient processing of Alzheimer's disease amyloid-Beta peptides by neuroectodermally converted mesenchymal stem cells. *Stem Cells Dev.* **19**, 629–633 (2010).
15. Lee, J. K. *et al.* Intracerebral transplantation of bone marrow-derived mesenchymal stem cells reduces amyloid-beta deposition and rescues memory deficits in Alzheimer's disease mice by modulation of immune responses. *Stem Cells.* **28**, 329–43 (2010).
16. Kil, J., Jin, H. K. & Bae, J. S. Bone marrow-derived mesenchymal stem cells reduce brain amyloid-beta deposition and accelerate the activation of microglia in an acutely induced Alzheimer's disease mouse model. *Neurosci. Lett.* **450**, 136–141 (2009).
17. Lee, H. J. *et al.* The therapeutic potential of human umbilical cord blood-derived mesenchymal stem cells in Alzheimer's disease. *Neurosci. Lett.* **481**, 30–35 (2010).
18. Zilka, N. *et al.* Mesenchymal stem cells rescue the Alzheimer's disease cell model from cell death induced by misfolded truncated tau. *Neuroscience* **193**, 330–337 (2011).
19. Katsuda, T., Kosaka, N., Takeshita, F. & Ochiya T. The therapeutic potential of mesenchymal stem cell-derived extracellular vesicles. *Proteomics* (in press).
20. Théry, C., Ostrowski, M. & Segura, E. Membrane vesicles as conveyors of immune responses. *Nat. Rev. Immunol.* **9**, 581–593 (2009).
21. Valadi, H. *et al.* Exosome-mediated transfer of mRNAs and microRNAs is a novel mechanism of genetic exchange between cells. *Nat. Cell Biol.* **9**, 654–659 (2007).
22. Taylor, D. D. & Gercel-Taylor, C. Exosomes/microvesicles: mediators of cancer-associated immunosuppressive microenvironments. *Semin. Immunopathol.* **33**, 441–454 (2011).
23. Kosaka, N. *et al.* Secretory mechanisms and intercellular transfer of microRNAs in living cells. *J. Biol. Chem.* **285**, 17442–17452 (2010).
24. Bruno, S. *et al.* Mesenchymal stem cell-derived microvesicles protect against acute tubular injury. *J. Am. Soc. Nephrol.* **20**, 1053–1067 (2009).
25. Lai, R. C. *et al.* Exosome secreted by MSC reduces myocardial ischemia/reperfusion injury. *Stem Cell Res.* **4**, 214–222 (2010).

26. Miners, J. S., Verbeek, M. M., Rikkert, M. O., Kehoe, P. G. & Love, S. Immunocapture-based fluorometric assay for the measurement of neprilysin-specific enzyme activity in brain tissue homogenates and cerebrospinal fluid. *J. Neurosci. Methods* **167**, 229–236 (2008).
27. Théry, C., Amigorena, S., Raposo, G. & Clayton, A. Isolation and characterization of exosomes from cell culture supernatants and biological fluids. *Curr. Protoc. Cell Biol.* Chapter 3:Unit 3.22 (2006).
28. Taylor, D. D., Zacharias, W. & Gercel-Taylor, C. Exosome isolation for proteomic analyses and RNA profiling. *Methods Mol. Biol.* **728**, 235–246 (2011).
29. Denzer, K., Kleijmeer, M. J., Heijnen, H. F., Stoorvogel, W. & Geuze, H. J. Exosome: from internal vesicle of the multivesicular body to intercellular signaling device. *J. Cell Sci.* **113**, 3365–3374 (2000).
30. Stewart, K. *et al.* STRO-1, HOP-26 (CD63), CD49a and SB-10 (CD166) as markers of primitive human marrow stromal cells and their more differentiated progeny: a comparative investigation in vitro. *Cell Tissue. Res.* **313**, 281–290 (2005).
31. van Niel, G., Porto-Carreiro, I., Simoes, S. & Raposo, G. Exosomes: a common pathway for a specialized function. *J. Biochem.* **140**, 13–21 (2006).
32. Shirotani, K. *et al.* Neprilysin degrades both amyloid beta peptides 1–40 and 1–42 most rapidly and efficiently among thiorphan- and phosphoramidon-sensitive endopeptidases. *J. Biol. Chem.* **276**, 21895–21901 (2001).
33. Trajkovic, K. *et al.* Ceramide triggers budding of exosome vesicles into multivesicular endosomes. *Science* **319**, 1244–1247 (2008).
34. Carlsson, L. *et al.* Characteristics of human prostasomes isolated from three different sources. *Prostate* **54**, 322–330 (2003).
35. Gatti, J. L., Métayer, S., Belghazi, M., Dacheux, F. & Dacheux, J. L. Identification, proteomic profiling, and origin of ram epididymal fluid exosome-like vesicles. *Biol. Reprod.* **72**, 1452–1465 (2005).
36. Conde-Vancells, J. *et al.* Candidate biomarkers in exosome-like vesicles purified from rat and mouse urine samples. *Proteomics* **4**, 416–425 (2010).
37. LaFerla, F. M., Green, K. N. & Oddo, S. Intracellular amyloid-beta in Alzheimer's disease. *Nat. Rev. Neurosci.* **8**, 499–509 (2007).
38. Keyser, K. A., Beagles, K. E. & Kiem, H. P. Comparison of mesenchymal stem cells from different tissues to suppress T-cell activation. *Cell Transplant* **16**, 555–562 (2007).
39. Banas, A. *et al.* IFATS collection: in vivo therapeutic potential of human adipose tissue mesenchymal stem cells after transplantation into mice with liver injury. *Stem Cells* **26**, 2705–2712 (2008).
40. Ahmadian, Kia N. *et al.* Comparative analysis of chemokine receptor's expression in mesenchymal stem cells derived from human bone marrow and adipose tissue. *J. Mol. Neurosci.* **44**, 178–185 (2011).
41. Ikegame, Y. *et al.* Comparison of mesenchymal stem cells from adipose tissue and bone marrow for ischemic stroke therapy. *Cytotherapy* **13**, 675–685 (2011).
42. Cocucci, E., Racchetti, G. & Meldolesi, J. Shedding microvesicles: artefacts no more. *Trends Cell Biol.* **19**, 43–51 (2009).
43. Alvarez-Erviti, L. *et al.* Delivery of siRNA to the mouse brain by systemic injection of targeted exosomes. *Nat. Biotechnol.* **29**, 341–345 (2011).
44. Zhuang, X. *et al.* Zhang HG.Treatment of brain inflammatory diseases by delivering exosome encapsulated anti-inflammatory drugs from the nasal region to the brain. *Mol. Ther.* **19**, 1769–1779 (2011).
45. Hemming, M. L. *et al.* Reducing amyloid plaque burden via ex vivo gene delivery of an Abeta-degrading protease: a novel therapeutic approach to Alzheimer disease. *PLoS Med.* **4**, e262 (2007).
46. Liu, Y. *et al.* Expression of neprilysin in skeletal muscle reduces amyloid burden in a transgenic mouse model of Alzheimer disease. *Mol. Ther.* **17**, 1381–1386 (2009).

Acknowledgements

We thank Drs. Takaomi Saido and Takashi Saito (RIKEN) for providing the N2a cells, Dr. Yukio Kato (Hiroshima University) for providing the human BM-MSCs #1 - #3, Dr. Yoko Kayama and Ms. Noriko Kai (Terabase Inc.) for providing electron microscopy images, Ms. Ayako Irie (Quantum Design Japan, Inc.) for assisting with NTA using the Nanosight system Mr. Ryushi Fukuda (Meiwafosis Co. Ltd) for assisting with the SIOS analysis using the q Nano system, and Ms. Ayako Inoue (National Cancer Center) for her excellent technical assistance. This study was supported in part by a Grant-in-Aid for the Third-Term Comprehensive 10-Year Strategy for Cancer Control of Japan, a grant-in-aid for Scientific Research on Priority Areas Cancer from the Japanese Ministry of Education, Culture, Sports, Science and Technology, a Grant-in-Aid for cancer research promotion from National Cancer Center of Japan, the Program for Promotion of Fundamental Studies in Health Sciences of the National Institute of Biomedical Innovation (NiBio) of Japan, and Grant-in-Aid for Scientific Research on Innovative Areas ("functional machinery for non-coding RNAs") from the Japanese Ministry of Education, Culture, Sports, Science, and Technology.

Author contributions

T.O. supervised the project; T.K., R.T., K.O., F.T., Y.S., M.K. and T.O. designed research; T.K., R.T., Y.Y. and K.T. performed experiments; T.K. and R.T. analyzed data; and T.K., N.K. and T.O. wrote the paper.

Additional information

Supplementary information accompanies this paper at http://www.nature.com/scientificreports

Competing financial interests: The authors declare no competing financial interests.

How to cite this article: Katsuda, T. *et al.* Human adipose tissue-derived mesenchymal stem cells secrete functional neprilysin-bound exosomes. *Sci. Rep.* 3, 1197; DOI:10.1038/srep01197 (2013).

Pharmaceuticals **2013**, *6*, 223-250; doi:10.3390/ph6020223

OPEN ACCESS

pharmaceuticals

ISSN 1424-8247

www.mdpi.com/journal/pharmaceuticals

Review

RNAi Therapeutic Platforms for Lung Diseases

Yu Fujita [1,2], Fumitaka Takeshita [1], Kazuyoshi Kuwano [2] and Takahiro Ochiya [1,*]

[1] Division of Molecular and Cellular Medicine, National Cancer Center Research Institute, Tokyo, 104-0045, Japan; E-Mails: yufujit2@ncc.go.jp (Y.F.); futakesh@ncc.go.jp (F.T.)

[2] Division of Respiratory Diseases, Department of Internal Medicine, Jikei University School of Medicine, Tokyo, 105-8461, Japan; E-Mail: kkuwano@jikei.ac.jp (K.K.)

* Author to whom correspondence should be addressed; E-Mail: tochiya@ncc.go.jp; Tel.: +81-3-3542-2511; Fax: +81-3-5565-0727.

Received: 19 December 2012; in revised form: 19 January 2013 / Accepted: 1 February 2013 / Published: 6 February 2013

Abstract: RNA interference (RNAi) is rapidly becoming an important method for analyzing gene functions in many eukaryotes and holds promise for the development of therapeutic gene silencing. The induction of RNAi relies on small silencing RNAs, which affect specific messenger RNA (mRNA) degradation. Two types of small RNA molecules, *i.e.* small interfering RNAs (siRNAs) and microRNAs (miRNAs), are central to RNAi. Drug discovery studies and novel treatments of siRNAs are currently targeting a wide range of diseases, including various viral infections and cancers. Lung diseases in general are attractive targets for siRNA therapeutics because of their lethality and prevalence. In addition, the lung is anatomically accessible to therapeutic agents via the intrapulmonary route. Recently, increasing evidence indicates that miRNAs play an important role in lung abnormalities, such as inflammation and oncogenesis. Therefore, miRNAs are being targeted for therapeutic purposes. In this review, we present strategies for RNAi delivery and discuss the current state-of-the-art RNAi-based therapeutics for various lung diseases.

Key words: RNAi; siRNA; miRNA; drug delivery system; lung diseases; lung cancer

---

1. Introduction

RNA interference (RNAi) is a natural endogenous mechanism for silencing gene expression that, recently, has been the focus of considerable attention for its potential use in new drugs [1]. The expression of a specific gene can be regulated using different mediators, such as short hairpin RNA

(shRNA), microRNA (miRNA), and small interfering RNA (siRNA). Gene silencing can be induced by siRNAs through a sequence-specific cleavage of perfectly complementary messenger RNA (mRNA); in contrast, miRNAs mediate translational repression and transcript degradation for imperfectly complementary targets. RNAi-based therapy may provide several advantages over conventional therapeutic approaches using small molecules, proteins, and monoclonal antibodies. Unlike traditional drugs, RNAi-based therapeutics can inhibit all classes of gene targets with high selectivity and potency, can provide personalized therapy, can be easily synthesized, and can be conducted through rapid steps of lead identification and optimization [2]. Synthetic oligonucleotides have other potential advantages, such as drug-like properties, that can often be improved through the introduction of chemical modifications, and manufacturing processes are usually amenable to scaled-up production. Several *in vivo* studies in animal models have demonstrated that RNAi-based therapeutics are effective for the treatment of various diseases, such as viral hepatitis [3], Huntington's disease [4], and some cancers [5]. Furthermore, there are several RNAi therapeutic agents in clinical development. Nevertheless, previous investigations have shown that there are several obstacles that need to be overcome before routine clinical applications are made. RNAi-based therapeutics are promptly degraded by nucleases when they are administered systemically, and chemical modifications at specific positions or formulation with delivery vectors have been shown to improve stability, but they may attenuate the suppressive activity of oligonucleotides [6]. Their systemic administration may induce undesirable off-target effects by activating the innate immune system via toll-like receptor (TLR)-dependent or independent mechanisms, leading to an increased number of inflammatory cytokines [7]. Success of the delivery of RNAi-based therapeutics necessitates efficiency, convenience, and patient compliance of the delivery route. For this reason, direct administration of RNAi-based therapeutics into the target organs is a promising approach for overcoming the problems of systemic administration. So far, an approach for drug treatment has been developed that includes transdermal, rectal, vaginal, and pulmonary drug delivery systems.

The lung is susceptible to many diseases because of its location and physiological function. It is usually exposed to many environmental pollutants, including smoke and volatile organic compounds, which lead to diseases such as asthma, emphysema, and lung cancer. Furthermore, many of the lethal infectious diseases are airborne and use the lungs as their main entrance to the body. Therefore, lung diseases have received particular attention as targets of direct administration of RNAi-based therapeutics. As a direct route to the lung, pulmonary delivery has offered a new method for the treatment of various lung diseases, such as cancer [8–12], respiratory infectious diseases [13–17], asthma [18,19], and pulmonary fibrosis [20,21]. The approach could potentially enhance the retention of RNAi-based therapeutics in the lungs and reduce systemic toxic effects. However, the development of pulmonary delivery for clinical applications remains a challenge for research of drug delivery systems and development. This review focuses on the latest development of pulmonary delivery and future plans for the RNAi-based treatment of various lung diseases.

2. Delivery of RNAi-Based Therapeutics to the Lungs

The lung is emerging as an attractive target for the treatment of various pathogenic disorders using RNAi-based therapeutics because of the increasing incidence of lung diseases with high mortality and

morbidity. The primary obstacle to translating RNAi-based therapy from the laboratories into the clinics is delivery. Delivery of siRNAs to the lungs is often studied and described using different routes and delivery strategies [22]; therefore, the focus of this chapter is on the characteristics of siRNA delivery to the lung.

In general, lung targeting can be achieved by intravenous as well as intrapulmonary administration. Although multiple routes of administration using siRNAs have been used, ranging from direct injection into target tissues to systemic administration, the use of siRNAs for the treatment of respiratory diseases has tended to focus on direct intratracheal or intranasal delivery of siRNAs to the lungs. The direct route offers several important benefits over systemic delivery, including the requirement for lower doses of siRNAs, the reduction of undesirable systemic side effects, and improved siRNA stability due to lower nuclease activity in the airways than in the serum. Lastly, and most importantly, in the context of treating respiratory disease, local administration of siRNAs allows direct access to lung epithelial cells, which are important cell types in a variety of pulmonary disorders [23]. Since the lung is accessible to therapeutic agents via multiple intrapulmonary routes, it has been a convenient model for *in vivo* validation of siRNA-mediated therapeutic gene silencing.

2.1. Pulmonary Delivery Approaches

Pulmonary delivery of therapeutic molecules, such as proteins and peptides, has been investigated for more than 30 years [23]. Pulmonary delivery can be achieved using intratracheal, intranasal, and inhalation routes. In most of the pulmonary siRNA therapy studies *in vivo*, siRNAs were delivered intratracheally or intranasally. In particular, intranasal delivery of siRNAs is widely used for administration due to its simplicity and adaptability to the delivery of various siRNA formulations, such as nasal spray and droplets. Although administration by inhalation is clinically the most common and non-invasive method to deliver therapeutic agents into the lung, only a few animal studies have been conducted on the formulation of inhalation of siRNAs [24,25].

2.1.1. Intratracheal and Intranasal Delivery

Intratracheal administration is one common method of pulmonary drug application. The pulmonary application method can be useful for the study of drug and vaccine delivery to the airway and lungs. Many animal studies have relied on intratracheal delivery of siRNAs to the lungs [15,26–31]. Moreover, some of them have also reported successful delivery of unmodified siRNAs without delivery vectors. The advantages of the intratracheal route are that it ensures high delivery efficiency with minimal loss of the drug and the application itself is quick and relatively inexpensive. The disadvantage is that, because it requires a surgical procedure, such as a tracheotomy, it is not a comfortable delivery method from the patient's viewpoint. With this method, the trachea is exposed during the procedure, and an endotracheal tube or microsyringe is inserted through an incision between the tracheal rings [Figure 1(a)]. This method is not routinely used for drug administration in humans [32]. On the other hand, Bivas-Benita *et al.* reported a relatively non-invasive pulmonary delivery via the endotracheal route [33]. In this method, the formulation is sprayed under anesthesia from the mouth to the trachea of mice using a microsyringe (Figure 1b). The main benefit of the endotracheal application is the visualization of the trachea, which is important for reliable lung administration. Compared with

traditional surgery, Bivas-Benita *et al.* reported that no mortality occurred as a result of the use of the endotracheal technique. Endotracheal applications are currently being used by many practitioners in the pulmonary field [22,34]; this is useful for studying pulmonary drug delivery in mice. However, the approach is more complex in humans because an artificial path for the delivery of drugs into the lungs is used. Therefore, the method is being used in animal models to test and evaluate its reliability for possible clinical applications.

Figure 1. Intratracheal route of siRNA administration into the lungs *in vivo* studies. (**a**) Intratracheal route: under anesthesia, the trachea is exposed surgically, and a tube or needle is inserted through an incision made between the tracheal rings. Complications, such as vascular injury and air leakage, are possible due to the tracheotomy. (**b**) Endotracheal route: siRNAs are sprayed directly from the mouth into the lungs using a MicroSprayer® aerolizer (Penn-Century, Philadelphia, PA, USA) and a laryngoscope. It is important to maintain a clear view of the trachea during the procedure.

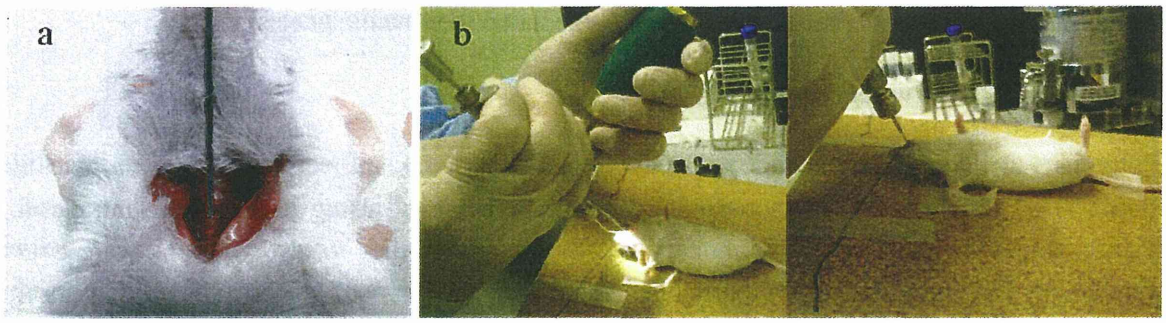

Intranasal delivery is another common method of pulmonary drug application in animal studies. In many studies, *in vivo* success has been demonstrated in delivering siRNAs to the lungs intranasally [22,35,36]. An experimental setup of intranasal delivery by spray or droplet is simple and painless for the animal. Although the success in delivering siRNAs intranasally in rodents cannot be completely extrapolated to human use because of the significant differences in lung anatomy [37], this approach has potential for the clinical application of siRNAs. Phase II clinical trials have been initiated for the treatment of respiratory syncytial virus (RSV) infection, making use of intranasal application of naked chemically modified siRNA molecules that target viral gene products [17,38] (see Section 3.1.1. for details).

Intranasal entry has long been used to administer small molecules, such as proteins, for systemic delivery. Because the nasal mucosa is highly vascularized, delivery of a thin epithelium of medication across the surface area can result in rapid absorption of the medication into the blood. Therefore, siRNAs administered intranasally might be deposited in the nose, and some of them may be unable to reach the lower respiratory tract. In fact, it has been reported that intranasal application of unformulated siRNAs resulted in lower delivery efficiency and homogeneous pulmonary distribution than that achieved with intratracheal application [31]. The intranasal method is suitable for some lung diseases, such as upper respiratory infection by RSV, and it also has potential for systemic delivery rather than pulmonary delivery of siRNAs. Therefore, it is important to consider the route of administration in animal studies when assessing the delivery and therapeutic efficacy of a formulation

for pulmonary delivery. Careful choice of efficient delivery in response to the condition of lung diseases is necessary.

2.1.2. Inhalation Delivery

The use of aerosols to deliver medication to the lungs has a long history. Administration by inhalation is a popular and non-invasive method of delivering agents into the lungs. There are several inhalation devices available for the delivery of drugs into the lungs. Metered dose inhalers (MDIs) and dry powder inhalers (DPIs) are the most common modes of inhaled delivery. MDIs are the most commonly used inhalers for several lung diseases, such as asthma, bronchitis, and chronic obstructive pulmonary disease (COPD), and a spacer is an external device that is attached to an MDI to allow for better drug delivery by enhanced actuation and inhalation coordination. For most MDIs, the propellant is one or more gases called chlorofluorocarbons (CFCs). Although CFCs in drugs are safe for patients to inhale, they are harmful to the environment. Therefore, further development of inhalable siRNAs may not be the best way forward. DPIs are devices that deliver medication to the lungs in the form of dry powder. The use of DPIs has already shown promise for the *in vivo* delivery of therapeutic macromolecules such as insulin [39] and low-molecular-weight heparin [40]; thus, it could be a better device for delivering siRNAs to the lungs. The advantages of DPIs are improved stability and sterility of biomolecules over liquid aerosols and propellant-free formation.

Although drugs are commonly delivered to the lungs by inhalation, most *in vivo* studies using siRNAs have relied on intratracheal or intranasal delivery. The reason could be the difficulty in formulating inhalable siRNAs and maintaining the stability during the delivery process. A suitable carrier is also needed to protect nucleic acids from degradation due to shear force and increased temperature during the drying process. The use of spray-drying as a technique for engineering dry powder formulations of siRNA nanoparticles, which might enable the local delivery of biologically active siRNA directly to the lung tissue, has been demonstrated [24,25]. In the future, the technique is desirable to estimate the *in vivo* study on siRNA therapy for inhalation. In the long term, we anticipate that there will be more sophisticated devices for clinical use and that those currently being developed will be more suitable.

2.2. Extracellular and Intracellular Barriers to siRNA Delivery

There are two main barriers to efficient pulmonary siRNA delivery to the cells of the lung. The first is the complex, branched anatomy of the lungs and biomechanical barriers, such as the mucus layer covering the airway cells [41,42] (Figure 2). A remarkable feature of the respiratory tract is its high degree of branching. Airway consists of respiratory bronchioles, alveolar ducts, and alveolar sacs. All of these structures bear alveoli, the tiny air sacs in which the gas exchange takes place. It is generally acknowledged that the critical factor for efficient siRNA delivery depends on the properties of RNAi drug particles in terms of size, charge, shape, velocity and density. For efficient pulmonary siRNA delivery, the particles must be deposited in the lower respiratory tract. Deposition in the airway is affected by the particle size and patient's pulmonary function. A particle size between 1–5 μm is found to be the most appropriate for deposition at the lower respiratory tract [23]. In addition, the presence of mucus and surfactant proteins, the mucociliary clearance actions, and phagocytosis by macrophages